Role of TAPP1 and TAPP2 adaptors binding to PtdIns(3,4)P2 in regulating insulin sensitivity defined by knock-in analysis

Stephan Wullschleger, David H Wasserman, Alex Gray, Kei Sakamoto, Dario R Alessi

Role of TAPP1 and TAPP2 adaptors binding to PtdIns(3,4)P_2 in regulating insulin sensitivity defined by knock-in analysis.

By
Stephan Wullschleger[1], David H. Wasserman[2], Alex Gray[3], Kei Sakamoto[1] and Dario R. Alessi[1]

1. MRC Protein Phosphorylation Unit, College of Life Sciences, University of Dundee, Dundee DD1 5EH, UK

2. Vanderbilt-NIH Mouse Metabolic Phenotyping Center, Vanderbilt University School of Medicine, Nashville, USA.

3. Division of Cell Signalling and Immunology, College of Life Sciences, University of Dundee, Dow Street, Dundee DD1 5EH, Scotland, U.K

Correspondence to SW (s.wullschleger@dundee.ac.uk) or DRA (d.r.alessi@dundee.ac.uk)

Telephone 44-1382, 344 241 Fax 44-1382, 223 778

Keywords: PH domain, PI 3-kinase, insulin signalling, tyrosine phosphatase PTPL1 and negative feedback loop

Running title: Analysis of non-PtdIns(3,4)P_2-binding TAPP1/TAPP2 knock-in mice

Abstract

Insulin sensitivity is critically dependent upon activity of PI 3-kinase and generation of the PtdIns(3,4,5)P_3 second messenger. PtdIns(3,4,5)P_3 can be broken down to PtdIns(3,4)P_2 through the action of the SHIP phosphatases. As PtdIns(3,4)P_2 levels peak after those of PtdIns(3,4,5)P_3, it has been proposed that PtdIns(3,4)P_2 controls a negative feedback loop that down-regulates the insulin and PI 3-kinase network. We previously identified two related adaptor proteins termed TAPP1 and TAPP2 that specifically bind to PtdIns(3,4)P_2 through their C-terminal PH domain. To determine whether TAPP1 and TAPP2 play a role in regulating insulin sensitivity, we generated knock-in mice that express normal endogenous levels of mutant TAPP1 and TAPP2 that are incapable of binding PtdIns(3,4)P_2. These homozygous TAPP1$^{R211L/R211L}$TAPP2$^{R218L/R218L}$ double knock-in mice are viable and exhibit significantly enhanced activation of the Akt kinase a key downstream mediator of insulin signalling. Consistent with increased PI 3-kinase and Akt activity the double knock-in mice display enhanced whole body insulin sensitivity and disposal of glucose uptake into muscle tissues. We also generated wild type and double TAPP1$^{R211L/R211L}$TAPP2$^{R218L/R218L}$ knock-in embryonic fibroblasts and found that insulin triggered enhanced production of PtdIns(3,4,5)P_3 and Akt activity in the double knock-in fibroblasts. These observations provide the first genetic evidence to support the notion that binding of TAPP1 and TAPP2 adaptors to PtdIns(3,4)P_2 functions to down-regulate the insulin and PI 3-kinase signalling pathways.

Introduction

The PI 3-kinase pathway plays a central role in regulating most cellular responses to insulin [1]. This is emphasised by the findings that marked insulin resistance is invariably induced by inhibiting the PI 3-kinase pathway in genetically modified animal models, or by administering inhibitors or employing high fat diets that suppress this signalling network [2, 3]. There is also ample evidence that insufficient PI 3-kinase pathway activation is a hallmark of type 2 diabetes in humans [2]. There is now good understanding of how activation of PI 3-kinase pathway controls insulin-signalling responses. Once activated by insulin, PI 3-kinase phosphorylates the D3 hydroxyl group of phosphatidylinositol(4,5) bisphosphate (PtdIns(4,5)P_2) to generate PtdIns(3,4,5)P_3, the key second messenger of the insulin-signalling pathway. PtdIns(3,4,5)P_3 triggers cellular responses to insulin by recruiting the Akt protein kinases that possess a PtdIns(3,4,5)P_3-binding PH domain to the plasma membrane. This induces a conformational change in Akt permitting its activation by the upstream PDK1 and mTORC2 protein kinases [4]. Once activated, Akt phosphorylates numerous substrates to regulate responses to insulin [5], including phosphorylating AS160 to stimulate glucose uptake [6] and GSK3 to promote glycogen synthesis [7].

The mechanisms that regulate the inactivation of the insulin-signalling pathway also play a vital role in regulating overall insulin actions. For example, over-activation of the mTORC1 pathway as a result of obesity induces insulin resistance by stimulating phosphorylation and degradation of insulin receptor substrate adaptor proteins required for activation of PI 3-kinase by insulin [8]. Furthermore, knock-out of the tyrosine phosphatase PTP1B that inactivates the insulin receptor, markedly sensitises mice to insulin and protects animals to developing insulin resistance when fed on a high fat diet [9]. The lipid phosphatases that breakdown PtdIns(3,4,5)P_3 also play vital roles in controlling sensitivity to insulin. For example, a modest 50% reduction in the expression of the PTEN phosphatase that converts PtdIns(3,4,5)P_3 to PtdIns(4,5)P_2, induces insulin sensitisation [10] and is sufficient to reverse marked insulin resistance in a mouse knock-in model in which the ability of the PDK1 kinase to interact with PtdIns(3,4,5)P_3 has been ablated [11]. PtdIns(3,4,5)P_3 can also be converted to PtdIns(3,4)P_2 by the SH2 containing inositol phosphatase-1 (SHIP1) and SHIP2 phosphatases [12, 13]. Mice lacking SHIP2 display enhanced activation of Akt following insulin administration and are highly resistant to weight gain when placed on a high-fat diet [14]. There has been much discussion whether PtdIns(3,4)P_2 functions as a signalling molecule in its own right as insulin and other agonists that activate the PI 3-kinase pathway significantly increase its levels [15]. Detailed analysis confirms that the majority of PtdIns(3,4)P_2 originates from PtdIns(3,4,5)P_3 and consistent with this levels of PtdIns(3,4)P_2 peak after PtdIns(3,4,5)P_3 [16].

To date numerous PH domain containing proteins have been identified that interact with PtdIns(3,4,5)P_3 specifically (GRP1, BTK, ARNO) or bind both PtdIns(3,4,5)P_3 and PtdIns(3,4)P_2 with similar affinity (Akt, PDK1, DAPP1) [15, 17]. However, to our knowledge the only proteins to have been identified that specifically interact with PtdIns(3,4)P_2 with high affinity are the Tandem PH containing Protein-1 (TAPP1) and TAPP2, related adaptor proteins consisting of two sequential PH domains in which the C-terminal PH domain binds PtdIns(3,4)P_2. The N-terminal PH domain does not interact with any lipid tested [18]. The structure of the C-terminal PH domain of TAPP1 suggested that several conserved basic residues interacted with the 3 and the 4 phosphate groups of PtdIns(3,4)P_2. Mutation of one of these residues, Arg211 on TAPP1 or the equivalent Arg218 residue in TAPP2, completely prevented interaction of these proteins with PtdIns(3,4)P_2 [18]. Binding of TAPP1 to PtdIns(3,4,5)P_3 is inhibited by steric hindrance of an Ala residue located close to the position in which the 5'-phosphate would be expected to reside [19]. Interestingly, the equivalent residue in PtdIns(3,4,5)P_3-binding PH domains is frequently a Gly. Mutation of the Ala residue to Gly in TAPP1 resulted in it being capable of interacting with PtdIns(3,4,5)P_3 and PtdIns(3,4)P_2 with similar affinity [19]. Evidence also suggests that TAPP1 binds PtdIns(3,4)P_2 selectively in vivo, as TAPP1 relocated from the cytosol to the plasma membrane of cells, following stimulation with agonists that induced PtdIns(3,4)P_2, but not with those that induced mainly PtdIns(3,4,5)P_3 [20]. Similarly, in B cells, both TAPP1 and TAPP2 translocated to the plasma membrane in response to antigen stimulation and this

correlated with the formation of PtdIns(3,4)P_2 rather than production of PtdIns(3,4,5)P_3 [21, 22].

The biological functions of TAPP1 and TAPP2 are not well characterised. Apart from the PH domains the only other known functional region is a C-terminal PDZ-binding motif that interacts with several PDZ binding proteins including the tyrosine-phosphatase-13 (PTPN13, previously known PTPL1 or FAP-1) [23] as well as the scaffolding proteins MUPP1 [20] syntrophin [24] and utrophin [25]. One hypothesis was that TAPP1 and TAPP2 by specifically recognising PtdIns(3,4)P_2 could function to recruit signalling molecules or complexes to the plasma membrane that down-regulate the PI 3-kinase signalling pathways [23]. As a first step to exploring this idea, we generated knock-in mice expressing point mutants of TAPP1 and TAPP2 unable to interact with PtdIns(3,4)P_2. The resulting TAPP1$^{R211L/R211L}$ TAPP2$^{R218L/R218L}$ double knock-in mice are viable and displayed significantly enhanced whole body insulin sensitivity in a hyperinsulinemic-euglycemic clamp study. We also demonstrate that TAPP1$^{R211L/R211L}$ TAPP2$^{R218L/R218L}$ double knock-in fibroblast cells display enhanced PtdIns(3,4,5)P_3 levels and Akt activation in response to insulin. Our data suggests that enhanced insulin sensitivity is mediated by increased Akt kinase activation thereby stimulating glucose uptake in heart and skeletal muscle. TAPP1$^{R211L/R211L}$ TAPP2$^{R218L/R218L}$ knock-in mice represent the first mouse model for these proteins and support the notion that TAPP1/TAPP2 operate as negative regulators of the PI 3-kinase signalling pathway.

Material and Methods

Materials and general buffers. Protein G–Sepharose and [γ^{32}P]-ATP were purchased from Amersham Pharmacia Biotech. Human insulin (Actrapid) from Novo-Nordisk was obtained from Ninewells Pharmacy, Dundee. PI-103 PI 3-kinase inhibitor [26] was synthesised by Natalia Shpiro (MRC Protein Phosphorylation Unit Dundee). Lysis buffer: 50 mM Tris-HCl pH 7.5, 1mM EDTA, 1 mM EGTA, 0.3% (w/v) CHAPS, 1 mM sodium orthovanadate, 50 mM sodium fluoride, 5 mM sodium pyrophosphate, 0.27 M sucrose, 0.1% (v/v) 2-mercaptoethanol and 'Complete' protease inhibitor cocktail (Roche).

Generation and genotyping of TAPP1$^{R211L/R211L}$ and TAPP2$^{R218L/R218L}$ knock-in mice. TaconicArtemis generated the TAPP1R211L/R211L and TAPP2R218L/R218L knock-in mice as described in the Fig1. The knock-in mice were generated and maintained on an inbred C57BL/6J background. Genotyping was performed by PCR using genomic DNA isolated from ear biopsies. For TAPP1 knock-in mice, Primer 1 (5'-CCTCATTCAGAGTATGCAGC-3') and Primer 2 (5'-CTACCTTCAAGGAAGTGTTCC-3'), and for TAPP2 knock-in mice, Primer 1 (5'- GGATGTTCTCAAGACTCACG-3') and Primer 2 (5'-CATCATGGGAGTAAGAGTAGG-3') were used to detect the wild-type and knock-in alleles. The PCR program consisted of 5 min at 95°C; 30 sec at 95°C; 30 sec at 60°C and 30 sec at 72°C: 35 cycles; 5 min at 72°C. DNA sequencing was performed by DNA Sequencing & Services (MRCPPU, College of Life Sciences, University of Dundee, Scotland, www.dnaseq.co.uk) using Applied Biosystems Big-Dye Ver 3.1 chemistry on an Applied Biosystems model 3730 automated capillary DNA sequencer.

Animals. Mice were maintained under specific pathogen-free conditions and all procedures were carried out in accordance with the regulations set by the University of Dundee and the United Kingdom Home Office.

Blood glucose and plasma insulin measurement. Blood glucose levels were determined using the Ascensia Breeze 2 blood glucose monitoring system (Bayer) following tail incision. For insulin measurement blood was collected from mice following tail incision and using Na-heparinised capillary tubes (Hawksley). The blood was centrifuged at 3000 x g for 15 min, and the supernatant collected. Plasma insulin levels were determined using a rat/mouse insulin ELISA kit from Millipore (No EZRMI-13K) according to the instructions of the manufacturer. Rat insulin ranging from 0 to 10 ng/ml was used as a standard.

PtdIns(3,4)P_2 - agarose pull-down. Mouse tissues were homogenised in 10 mM HEPES (pH 7.4), 150 mM NaCl, 0.25% NP40, 1 mM benzamidine, 0.1 mM PMSF and 2 mM sodium orthovanadate. Tissue lysates were centrifuged at 18000 x g for 15 min at 4°C and the supernatant was snap frozen and stored at -80°C. 1 mg of tissue lysate was incubated with 25 µl of PtdIns(3,4)P_2 PIP beads (Echelon) for 1.5 hrs at 4°C. Beads were washed 3 times with 10 mM HEPES (pH 7.4), 150 mM NaCl, 0.25% NP40 and proteins were eluted with SDS-PAGE sample buffer (250 mM Tris pH 6.8, 5% SDS, 5% 2-mercaptoethanol, 32.5% glycerol) at 95°C for 5 min. Eluted proteins were analysed by immunoblotting.

Antibodies. The following antibodies were raised in sheep and affinity purified on the appropriate antigen. The total antibody used for immunoprecipitation and immunoblotting of Akt1 (S742B, 3rd bleed) was raised against full length His-Akt1. The TAPP1 antibody (S022C, 2nd bleed) was raised against residues 252-356 of mouse GST-TAPP1. The TAPP2 antibody (S392A, 1st bleed) was raised against residues 396-415 of mouse GST-TAPP2. The PRAS40 antibody (S115B, 1st bleed) was raised against the sequence DLPRPRLNTSDFQKLKRKY corresponding to residues 238-256 of human PRAS40. An antibody that recognizes PRAS40 phosphorylated at Thr246 (S114B, 2nd bleed) was raised against the peptide CRPRLNpTSDFQK. The FOXO1 antibody (S457, 3rd bleed) was raised against GST-FOXO1 comprising residues 2-655 of human FOXO1. The Akt p-Thr308 (#9275), Akt p-Ser473 (#9271), FOXO1 p-Thr24 (#9464), GSK3α/β p-Ser21/p-Ser9 (#9331) were purchased from Cell Signaling Technology. The GSK3α/β antibody (#44-610) was purchased from Biosource. The IRS1 antibody (06-248) was from Millipore and the IRS1 p-

Tyr612 antibody (44-816G) was purchased from Invitrogen. The GAPDH antibody (ab8245) was purchased from Abcam. Detection of immune complexes was performed using either fluorophore-conjugated secondary antibodies (Molecular Probes) followed by visualisation using an Odyssey® LI-COR imaging system or by HRP (horseradish peroxidase)-conjugated secondary antibodies (Pierce) and an enhanced chemiluminescence reagent.

Preparation of tissue lysates, immunoblotting and Akt kinase assay. Following a 5 hour fast, a bolus of insulin (1 mU/g body weight) was intravenously injected through the inferior vena cava to mice that had been terminally anaesthetised by pentobarbital (86 μg/ g body weight, intraperitoneally injected). After 20 min tissues (heart, liver, gastrocnemius muscle) were extracted, frozen in liquid nitrogen and stored at -80°C. Tissues were homogenised on ice in a 10-fold mass excess of ice-cold lysis buffer using a Kinematica Polytron. Tissue lysates were centrifuged at 18000 x g for 15 min at 4°C and the supernatant was snap frozen and stored at -80°C. Lysates (20 μg) were analysed by immunoblotting using the antibodies, as indicated in the figure. The activity of Akt1 was assessed either by immunoblotting of tissue lysate (20 μg) or by kinase activity assays. Briefly, Akt1 was immunoprecipitated from 1 mg of tissue lysate and kinase activity was measured using the Crosstide peptide (GRPRTSSFAEG) as described previously [27]. Values of Akt activity were given as mean±SEM for the number of mice indicated in the figure legends and significance was determined by unpaired two-tailed *t* tests.

Generation and stimulation of mouse embryonic fibroblasts. Mouse embryonic fibroblasts isolated from day 13.5 mouse embryos were generated as previously described [28] and immortalised by continuous passaging. Cells were cultured in Dulbecco modified Eagle medium (DMEM) containing 10% serum (Sigma), 2 mM L-glutamine, 50 U of penicillin G/ml, and 50 μg of streptomycin/ml (Life Technologies). Cells were serum-starved in DMEM with L-glutamine, penicillin and streptomycin for 16 hrs before stimulation. Cells were stimulated with insulin (10 nM) for 15 min and 30 min. Cells were subsequently lysed in lysis buffer and the lysates were centrifuged at 18000 x g for 15 min at 4°C. The supernatant was snap frozen and stored at -80°C. Lysates (10 μg) were analysed by immunoblotting using the antibodies, as indicated in the figure.

Hyperinsulinemic-euglycemic clamp studies. Male mice at 6 months of age were used for a hyperinsulinemic-euglycemic clamp studies were performed at Vanderbilt-NIH Mouse Metabolic Phenotyping Center, Nashville, USA, as previously described in detail [29]. Catheters were implanted in a carotid artery and a jugular vein of mice for sampling and infusions, respectively, 5 days prior to study [30]. Insulin clamps were performed on 5 hr fasted mice [29]. [3-^{3}H]glucose was primed (2.4 μCi) and continuously infused for a 90-min equilibration period (0.04 μCi/min) and a 2 hr clamp period (0.12 μCi/min). Baseline blood or plasma parameters were determined as the mean of values obtained in blood samples collected at -15 and -5min. At time 0, insulin infusion (4 mU·kg^{-1}·min^{-1}) was started and continued for 165 min. Blood glucose was clamped at 150~160 mg/dL using a variable rate of glucose infusion (GIR). Mice received heparinised saline-washed erythrocytes from donors at 5 μL/min to prevent a fall of hematocrit. Insulin clamps were validated by assessment of blood glucose over time. Blood glucose was monitored every 10 min and the GIR was adjusted as needed. Blood was taken at 80-120 min for the determination of [3-^{3}H]glucose. Clamp insulin was determined at t=100 and 120 min. At 120 min, 13 μCi of 2[^{14}C]deoxyglucose ([^{14}C]2DG) was administered as an intravenous bolus. Blood was taken at 122, 125, 130, and 135 min for the determination of [^{14}C]2DG. After the last sample, mice were anesthetised and tissues were collected.
Plasma insulin was determined by ELISA (Millipore). Non-esterified fatty acids were assayed enzymatically using the Wako Diagnostics. Radioactivity of [3-^{3}H]glucose, [^{14}C]2DG, and [^{14}C]2DG-6-phosphate in plasma and tissue samples were determined by liquid scintillation counting [30]. Whole body glucose appearance (R_a) and disappearance (R_d) rates were determined using non-steady-state equations [31], EndoR_a was determined by subtracting the GIR from total R_a. Glucose uptake was calculated as previously described [32].

The area under the curve was calculated using GraphPad PRISM software. Values were given as mean±SEM for the number of mice indicated in the figure legends. Significance was determined by unpaired two-tailed *t* tests.

Measurement of PtdIns(3,4,5)P_3 levels. This was undertaken employing a time resolved fluorescence resonance energy transfer (TR-FRET) displacement assay that was described previously [33]. Briefly, wild type or knock-in mouse embryonic fibroblasts cultured on 10 cm diameter dishes were deprived of serum overnight and then left untreated in the absence or presence of 1 μM PI 103 or stimulated with insulin (10 nM) for the indicated times. Cells were lysed by incubation with 1.5 ml of ice-cold 0.5 M trichloroacetic acid. Cells were then pelleted by centrifugation (13, 000 x g for 1 min) and non-charged lipids extracted by washing cell pellets with 1 ml of a neutral solvent (methanol chloroform 2:1) for 20 min. PtdIns(3,4,5)P_3 was extracted by washing with 0.5 ml of an acidic solvent (methanol:chloroform:12 M HCl 80:40:1) for 20 min. The acidic extract containing PtdIns(3,4,5)P_3 was phase split by addition of 0.18 ml chloroform and 0.3 ml 0.1M HCl. After centrifugation, the lower organic phase containing PtdIns(3,4,5)P_3, was collected and dried under vacuum. The lipid pellet was re-suspended by sonication (15 sec 40 W in a cup sonicator bath) in 0. 06 ml TRFRET assay buffer consisting of 50 mM TRIS/HCl pH 7.4, 0.15 M NaCl, 0. 1 mM EDTA, 0.1 mM EGTA, 2m M DTT and 1.2% (w/v) Sodium Cholate. Duplicate 25 μl samples were assayed for PtdIns(3,4,5)P_3 content in the previously described TR-FRET displacement assay [33]. The estimated PtdIns(3,4,5)P_3 levels were normalised to cell density by estimating protein levels in the extracted cell pellets. This was achieved by recovering cells from the upper phase of the phase split material by the addition of 1ml of acetone (to remove residual chloroform) and centrifugation. The air-dried pellets were then dissolved overnight by gentle shaking in 0.2 M NaOH 1% (w/v) SDS at 50 ^{o}C. Protein in the dissolved pellets was estimated by Micro BCA protein assay kit (Thermo Scientific) according to the manufacturers instructions.

Results

Generation and analysis of TAPP1$^{R211L/R211L}$ and TAPP2$^{R218L/R218L}$ knock-in mice. To study the physiological role of TAPP1 and TAPP2, we generated knock-in mice in which the critical Arg residues required for PtdIns(3,4)P_2-binding (Arg211 of TAPP1 and Arg218 of TAPP2 [18, 19]) were mutated to Leu in order to abolish the ability of these adaptors to interact with phosphoinositides. The strategy to generate and genotype the TAPP1$^{R211L/R211L}$ and TAPP2$^{R218L/R218L}$ knock-in mice is summarised in Figure 1. The knock-in mice were generated and maintained on an inbred C57BL/6J background.

Single TAPP1$^{R211L/R211L}$ or TAPP2$^{R218/R218L}$ or double TAPP1$^{R211L/R211L}$ TAPP2$^{R218L/R218L}$ were viable and born at the expected Mendelian frequency (Table 1). The strategy used to breed wild-type TAPP1$^{+/+}$ TAPP2$^{+/+}$ control and experimental TAPP1$^{R211L/R211L}$ TAPP2$^{R218L/R218L}$ double knock-in mice is outlined in Table 1. The TAPP1 and TAPP2 proteins were expressed at the same levels in all tissues examined of wild-type TAPP1$^{+/+}$ TAPP2$^{+/+}$ and homozygous TAPP1$^{R211L/R211L}$ TAPP2$^{R218L/R218L}$ double knock-in mice, establishing that mutation does not affect protein stability (Fig 2A). TAPP1 (Fig 2B) and TAPP2 (Fig 2C) proteins derived from wild-type TAPP1$^{+/+}$ TAPP2$^{+/+}$ tissues but not those from TAPP1$^{R211L/R211L}$ TAPP2$^{R218L/R218L}$ double knock-in tissues interacted with agarose resin conjugated to PtdIns(3,4)P_2, confirming that the knock-in mutation ablated the ability of TAPP1 and TAPP2 to interact with PtdIns(3,4)P_2. The TAPP1$^{R211L/R211L}$ TAPP2$^{R218L/R218L}$ double knock-in mice compared to wild-type TAPP1$^{+/+}$ TAPP2$^{+/+}$ mice displayed normal body weight (Fig 2D) as well as fed and fasted levels of blood glucose (Fig 2E) and plasma insulin (Fig 2F). We have maintained the double knock-in mice over a 14-month period and no discernable overt phenotype was noted.

Increased activation of Akt in TAPP1$^{R211L/R211L}$ TAPP2$^{R218L/R218L}$ double knock-in mice. To investigate how inhibiting the ability of TAPP1 and TAPP2 to interact with PtdIns(3,4)P_2 impacts on the insulin signalling pathway, we injected mice deprived of food for 5 hrs with insulin (1 mU/g body weight) and analysed phosphorylation and activation of Akt in various insulin responsive tissues, including liver (Fig 3A), heart (Fig 3B) and gastrocnemius skeletal muscle (Fig 3C). We observed that there was no difference in the basal Akt activity between wild-type TAPP1$^{+/+}$ TAPP2$^{+/+}$and TAPP1$^{R211L/R211L}$ TAPP2$^{R218L/R218L}$ double knock-in mice, whereas insulin-stimulated Akt activation was significantly enhanced in tissues derived from insulin-injected TAPP1$^{R211L/R211L}$ TAPP2$^{R218L/R218L}$ double knock-in compared to wild-type TAPP1$^{+/+}$ TAPP2$^{+/+}$ animals (Fig 3 A to C). Increased activation of Akt in TAPP1$^{R211L/R211L}$ TAPP2$^{R218L/R218L}$ double knock-in mice was accompanied by enhanced phosphorylation of Akt at Thr308 (PDK1 site) and Ser473 (mTORC2 site) activating residues. Quantitative immunoblotting analysis confirmed that insulin stimulation of double knock-in mice induced a statistically significant increase in Thr308 and Ser473 phosphorylation in heart and gastrocnemius tissues (Supplementary Fig 1). Despite enhancement of Akt activity, this was not translated into a significant increase in the phosphorylation of Akt substrates examined (PRAS40, GSK3α/β and Foxo-1). Moreover, no marked changes were observed in IRS1 phosphorylation at Tyr612 (Fig 4A-C), a key-binding site for PI 3-kinase, which is phosphorylated by the insulin receptor [34]. This is considered further in the discussion.

Enhanced whole body insulin sensitivity in TAPP1$^{R211L/R211L}$ TAPP2$^{R218L/R218L}$ double knock-in mice. To investigate whether increased insulin-induced activation of Akt in the TAPP1$^{R211L/R211L}$ TAPP2$^{R218L/R218L}$ double knock-in mice enhanced insulin sensitivity in the most physiological context, we performed hyperinsulinemic-euglycemic clamp, a method that is considered the gold standard for assessing insulin actions on whole body glucose homeostasis in vivo [35], on TAPP1$^{R211L/R211L}$ TAPP2$^{R218L/R218L}$ double knock-in mice and wild-type TAPP1$^{+/+}$ TAPP2$^{+/+}$ control mice. These studies were undertaken at the Vanderbilt NIH Mouse Metabolic Phenotyping Center (http://www.mc.vanderbilt.edu/MMPC/) and we employed the clamp study in conscious and unrestrained animals [29]. Blood glucose levels were maintained by a variable glucose infusion during a 4 mU·kg^{-1}·min^{-1} constant rate insulin infusion (Suppl Fig 2A). Interestingly, the key index of whole body insulin sensitivity, glucose infusion rate required to maintain euglycemia, was increased at all time points in TAPP1$^{R211L/R211L}$ TAPP2$^{R218L/R218L}$ double knock-in mice compared to wild-type TAPP1$^{+/+}$ TAPP2$^{+/+}$ control mice (Fig 4A). Calculation of the area under the curve during establishment

of the clamp between 80 min and 120 min revealed significantly higher (25%) glucose infusion rate in TAPP1$^{R211L/R211L}$ TAPP2$^{R218L/R218L}$ double knock-in mice compared to wild-type TAPP1$^{+/+}$ TAPP2$^{+/+}$ control mice. The steady state whole body glucose disappearance rate (R_d) during the clamp was also significantly higher (23%) in TAPP1$^{R211L/R211L}$ TAPP2$^{R218L/R218L}$ double knock-in mice in comparison to wild-type TAPP1$^{+/+}$ TAPP2$^{+/+}$ mice (Fig 4B).

These results demonstrate that TAPP1$^{R211L/R211L}$ TAPP2$^{R218L/R218L}$ double knock-in mice display significantly enhanced whole body insulin sensitivity measured in conscious, unrestrained animals in vivo. Endogenous glucose appearance (EndoR_a) is the sum of hepatic glycogenolysis and gluconeogenesis in the post-absorptive state. In the basal state EndoR_a was comparable in TAPP1$^{R211L/R211L}$ TAPP2$^{R218L/R218L}$ double knock-in mice and wild-type TAPP1$^{+/+}$ TAPP2$^{+/+}$ mice. EndoR_a was suppressed equally in both genotypes during insulin clamps (Fig 4C). EndoR_a therefore did not account for the enhanced insulin sensitivity observed in TAPP1$^{R211L/R211L}$ TAPP2$^{R218L/R218L}$ double knock-in mice. The optimal insulin dose used to examine liver is much lower than the optimal insulin dose used to examine muscle. The insulin dose used was specifically chosen to amplify an insulin effect on glucose flux in cardiac and skeletal muscle. EndoR_a was maximally suppressed and therefore an enhanced effect at the liver could not be elucidated. Considering the elevated Akt activation in TAPP1$^{R211L/R211L}$ TAPP2$^{R218L/R218L}$ double knock-in mice it is very possible that an enhanced insulin suppression of EndoR_a would have been observed at a lower insulin dose (<2.0 $mU \cdot kg^{-1} \cdot min^{-1}$). In addition, non-esterified fatty acid concentrations were comparable in wild-type TAPP1$^{+/+}$ TAPP2$^{+/+}$ and TAPP1$^{R211L/R211L}$ TAPP2$^{R218L/R218L}$ double knock-in mice, indicating that insulin's effect on lipolysis was similar between the two genotypes (Suppl Fig 2B). Glucose uptake measured by infusion of [^{14}C]-2-deoxyglucose during the steady state phase of the clamp revealed comparable glucose uptake into adipose and diaphragm of wild-type TAPP1$^{+/+}$ TAPP2$^{+/+}$ and TAPP1$^{R211L/R211L}$ TAPP2$^{R218L/R218L}$ double knock-in mice (Fig 4D). Interestingly, significant increases of rates of glucose uptake in gastrocnemius muscle (77% increase) and heart (75% increase) of TAPP1$^{R211L/R211L}$ TAPP2$^{R218L/R218L}$ were detected in double knock-in mice in comparison to wild-type TAPP1$^{+/+}$ TAPP2$^{+/+}$ mice in which we also found increased activation of Akt (Fig 3). As is often the case in insulin sensitive mice [30], the basal and clamp insulin levels are reduced. This is important to consider since the increased insulin action was observed in the TAPP1$^{R211L/R211L}$ TAPP2$^{R218L/R218L}$ double knock-in mice despite reduced insulin concentrations (Suppl Fig 2C). These results indicate that the enhanced whole body insulin sensitivity observed in TAPP1$^{R211L/R211L}$ TAPP2$^{R218L/R218L}$ double knock-in mice is likely mediated through increased glucose uptake into skeletal muscle and heart tissues.

Increased levels of PtdIns(3,4,5)P_3 and Akt activation in TAPP1$^{R211L/R211L}$ TAPP2$^{R218L/R218L}$ knock-in fibroblasts. We generated immortalised mouse embryonic fibroblasts derived from wild-type TAPP1$^{+/+}$ TAPP2$^{+/+}$ and TAPP1$^{R211L/R211L}$ TAPP2$^{R218L/R218L}$ double knock-in E13.5 stage embryos. These cells were stimulated with 10 nM insulin for various time points and PtdIns(3,4,5)P_3 levels measured employing a previously described TR-FRET assay [33]. This revealed similar levels of PtdIns(3,4,5)P_3 in non-stimulated wild type and or double knock-in cells (Fig 5A). There was also no marked difference in PtdIns(3,4,5)P_3 levels between cells treated with the PI 3-kinase PI103 inhibitor. However, following insulin stimulation, at all time points examined, we observed a 1.5 to 2-fold increase in PtdIns(3,4,5)P_3 levels in the TAPP1$^{R211L/R211L}$ TAPP2$^{R218L/R218L}$ cells compared to TAPP1$^{+/+}$ TAPP2$^{+/+}$ fibroblasts (Fig 5A). We also observed that Akt was phosphorylated and activated to a significantly greater extent in TAPP1$^{R211L/R211L}$ TAPP2$^{R218L/R218L}$ double knock-in fibroblasts compared to wild-type TAPP1$^{+/+}$ TAPP2$^{+/+}$ cells (Fig 5B). Moreover, unlike in mouse tissues we observe that the TAPP1$^{R211L/R211L}$ TAPP2$^{R218L/R218L}$ double knock-in fibroblasts stimulated with insulin, display a modest increase in the phosphorylation of PRAS40 and GSK3α/β compared to wild-type TAPP1$^{+/+}$ TAPP2$^{+/+}$ cells (Fig 5B).

Discussion

The key finding of this study is that the TAPP1$^{R211L/R211L}$ TAPP2$^{R218L/R218L}$ double knock-in mice display significantly enhanced whole body insulin sensitivity. This provides the first genetic evidence establishing that the TAPP1 and TAPP2 adaptor proteins regulate insulin sensitivity by binding to PtdIns(3,4)P_2. Our data from *in vivo* clamp studies suggest that insulin sensitivity results from increased glucose disposal into heart and skeletal muscle. This is supported by the 1.5 to 2-fold increase in activity of Akt which is well-known to control glucose transport in response to insulin [36]. The increased activation of Akt observed in TAPP1$^{R211L/R211L}$ TAPP2$^{R218L/R218L}$ knock-in mice is likely to result from enhanced activation of PI 3-kinase that would account for the increased phosphorylation of Akt at Thr308 (PDK1 T-loop site) and Ser473 (mTORC2 site, hydrophobic motif) (Fig 3). This increased Akt phosphorylation and activation is also observed in fibroblasts derived from TAPP1$^{R211L/R211L}$ TAPP2$^{R218L/R218L}$ double knock-in embryos (Fig 5B). Overall these findings support the notion that binding of TAPP1 and TAPP2 to PtdIns(3,4,)P_2 results in down-regulation of PI 3-kinase and the insulin-signalling pathway.

It should be noted that the increased activation of Akt observed in TAPP1 and TAPP2 double knock-in mice did not lead to marked increase in the phosphorylation of Akt substrates that we have analysed (PRAS40, GSK3, Foxo) in various insulin responsive tissues (Fig 3). Similar results have been obtained in other studies where marked alterations in insulin sensitivity were correlated with changes in Akt activity, which were not reflected by monitoring phosphorylation of PRAS40, GSK3 or Foxo. For example, knock-in mutation of the PDK1 PH domain to prevent interaction with PtdIns(3,4,5)P_3 in mice, results in a ~2-fold inhibition of Akt resulting in marked insulin resistance, without significantly affecting the phosphorylation of Akt substrates [11, 37]. This lack of effect on phosphorylation of Akt substrates is likely to be a result from the inherent spare capacity and amplification of signalling pathways. These data suggest that in vivo insulin sensitivity can be intricately correlated with Akt activation and even modest 1.5 to 2-fold changes in Akt activity are sufficient to induce profound changes in insulin sensitivity. More work needs to be undertaken to identify the key substrates that Akt phosphorylates to regulate insulin sensitivity and how modest changes in Akt activity influences this process. It is also likely that PtdIns(3,4,5)P_3 will stimulate other Akt independent pathways that modulate overall insulin sensitivity.

It makes sense to employ PtdIns(3,4)P_2 as a signal to down-regulate the PI 3-kinase pathway, as the levels of this 3-phosphoinositide peaks later than PtdIns(3,4,5)P_3. PtdIns(3,4)P_2 would serve to down-regulate PI 3-kinase and signal the need for decreased formation of PtdIns(3,4,5)P_3 production. Functionally this would accelerate the return of insulin action to the pre-fed state. Further evidence supporting the notion that PtdIns(3,4)P_2 acts as a negative regulator of the PI 3-kinase pathway is provided by analysis of SHIP2 knock-out mice. Mice lacking the SHIP2 phosphatase that converts PtdIns(3,4,5)P_3 to PtdIns(3,4)P_2 displayed similar increased Akt activation in response to insulin in liver and muscle, as we have found in the TAPP1$^{R211L/R211L}$ TAPP2$^{R218L/R218L}$ double knock-in mice [14]. These results have been interpreted to result from increased levels of PtdIns(3,4,5)P_3 in the SHIP2 knock-out mice leading to increased activation of Akt. However, it would be interesting to explore whether the increased activation of Akt results instead from diminished recruitment of the TAPP1/TAPP2 adaptor proteins to the plasma membrane as a result of decreased levels of PtdIns(3,4)P_2 being produced in SHIP2 knock-out mice. SHIP1/SHIP2 phosphatases have also been implicated in playing roles in negatively regulating the PI 3-kinase pathway in immune cells [38]. The activity of the SHIP1/SHIP2 phosphatases is exquisitely controlled by interaction with growth factor receptors and by phosphorylation of tyrosine residues [39]. Presumably being able to intricately regulate the activity of the SHIP Phosphatases is vital, as they play dual roles in directly controlling absolute levels of PtdIns(3,4,5)P_3, as well as acting as gatekeepers of PtdIns(3,4)P_2 production that could in turn influence PI 3-kinase signalling networks via recruitment of the TAPP1/TAPP2 adaptors.

An important question for future research is to define the mechanism by which recruitment of TAPP1 and TAPP2 to plasma membrane down-regulates the PI 3-kinase pathway. Thus far

TAPP1 and TAPP2 have been reported to interact via their C-terminal residues with at least three PDZ domain binding proteins including the tyrosine-phosphatase-13 (PTPN13, previously known PTPL1 or FAP-1) [23] as well as the scaffolding proteins MUPP1 [20], syntrophin [24] and utrophin [25]. PTPN13 [40], MUPP1 [41], syntrophin and utrophin [42] are known to interact with a large number of binding partners involved in regulating numerous signalling pathways, so it may not be straightforward to deconvolute which of these is involved in regulating insulin-sensitivity. It is also possible that TAPP1/TAPP2 bind to other regulators of the PI 3-kinase pathway that have not been identified. PTPN13 is an attractive candidate to be a mediator of PI 3-kinase pathway signalling as the three dimensional structure of PTPN13 closely resembles the structure of PTP1B, one of the physiological tyrosine phosphatases that acts on the insulin receptor [43]. PTPN13 contains a positively charged pocket located near the catalytic site, reminiscent of the second phosphotyrosine binding site in PTP1B, which is required to dephosphorylate peptides containing two adjacent phosphotyrosine residues as occurs for example in the activated insulin receptor [44]. Consistent with this PTPN13, like PTP1B, interacted with and dephosphorylates a di-phosphorylated insulin receptor peptide much more efficiently than mono-phosphorylated peptides. This indicates that PTPL1 may down-regulate the PI 3-kinase pathway by dephosphorylating the insulin or potentially other growth factor receptors that contain tandem phosphotyrosines [43]. We have generated catalytically inactive PTPN13$^{C2374A/C2374A}$ knock-in mice. These mice are viable and in initial studies do not appear to display marked insulin sensitisation (SW and DRA, unpublished work), suggesting that PTPN13 may not be a rate-limiting in the mechanism by which TAPP1/TAPP2 proteins control insulin sensitivity. In future work, it would be important to study which proteins are associated with TAPP1 and TAPP2 in insulin-responsive tissues and evaluate whether these are involved in down regulating insulin signalling when recruited to the plasma membrane.

In conclusion, the TAPP1$^{R211L/R211L}$ TAPP2$^{R218L/R218L}$ knock-in mice represent the first mouse model for these adaptor proteins and support the notion that TAPP1/TAPP2 operate as negative regulators of the PI 3-kinase signalling pathway. As TAPP1 and TAPP2 are expressed in all tissues examined these adaptors may have roles to play in modulating PI 3-kinase activity and PtdIns(3,4,5)P_3 levels in systems beyond controlling insulin sensitivity. In future work it would be important to define the mechanism by which TAPP1 and TAPP2 proteins induce down-regulation of the PI 3-kinase by binding to PtdIns(3,4)P_2 and establish whether this system plays more general roles in other biological systems, such as in B-cells and T-cells where TAPP1/TAPP2 proteins are highly expressed. These results also indicate that if compounds could be developed that inhibit binding of TAPP1 and TAPP2 to PtdIns(3,4)P_2, these could be deployed to improve insulin sensitivity in insulin resistant diabetic patients. Interestingly, a recent study has shown that it is possible to design small molecules that bind to the 3-phosphoinositide binding sites of PH domains [45] and it would be interesting to employ a similar approach to develop compounds that prevent TAPP1/TAPP2 binding to PtdIns(3,4)P_2. It would also be important to identify the proteins that interact with TAPP1 and TAPP2 to control insulin sensitivity as these might also represent new therapeutic targets for the treatment of insulin resistance.

Acknowledgments
We acknowledge Gail Fraser for genotyping of mice, the Sequencing Service (School of Life Sciences, University of Dundee, Scotland) for DNA sequencing coordinated by Nicholas Helps, the protein production and antibody purification teams [Division of Signal Transduction Therapy (DSTT), University of Dundee] co-ordinated by Hilary McLauchlan and James Hastie for generation of antibodies. We thank the Medical Research Council and the pharmaceutical companies supporting the Division of Signal Transduction Therapy Unit (AstraZeneca, Boehringer-Ingelheim, GlaxoSmithKline, Merck KgaA and Pfizer) for financial support. The research was also supported by NIH grants U24 DK059637 and R01 DK054902. Surgery and clamps were performed by Bingle Bracy and Dr. Li Kang of Vanderbilt University School of Medicine.

Author contributions
SW undertook most of the experimentation, KS provided key expertise with mice studies and helped with insulin injections, DHW undertook the clamp studies and AG undertook PtdIns(3,4,5)P_3 measurements. All authors were involved in planning and analysing the experimental data. SW and DRA wrote the manuscript.

References

1 Taniguchi, C. M., Emanuelli, B. and Kahn, C. R. (2006) Critical nodes in signalling pathways: insights into insulin action. Nat Rev Mol Cell Biol. **7**, 85-96

2 Biddinger, S. B. and Kahn, C. R. (2006) From mice to men: insights into the insulin resistance syndromes. Annu Rev Physiol. **68**, 123-158

3 Ihle, N. T., Paine-Murrieta, G., Berggren, M. I., Baker, A., Tate, W. R., Wipf, P., Abraham, R. T., Kirkpatrick, D. L. and Powis, G. (2005) The phosphatidylinositol-3-kinase inhibitor PX-866 overcomes resistance to the epidermal growth factor receptor inhibitor gefitinib in A-549 human non-small cell lung cancer xenografts. Mol Cancer Ther. **4**, 1349-1357

4 Pearce, L. R., Komander, D. and Alessi, D. R. (2010) The nuts and bolts of AGC protein kinases. Nat Rev Mol Cell Biol. **11**, 9-22

5 Manning, B. D. and Cantley, L. C. (2007) AKT/PKB signaling: navigating downstream. Cell. **129**, 1261-1274

6 Sakamoto, K. and Holman, G. D. (2008) Emerging role for AS160/TBC1D4 and TBC1D1 in the regulation of GLUT4 traffic. Am J Physiol Endocrinol Metab. **295**, E29-37

7 McManus, E. J., Sakamoto, K., Armit, L. J., Ronaldson, L., Shpiro, N., Marquez, R. and Alessi, D. R. (2005) Role that phosphorylation of GSK3 plays in insulin and Wnt signalling defined by knock-in analysis. EMBO J. **24**, 1571-1583

8 Um, S. H., Frigerio, F., Watanabe, M., Picard, F., Joaquin, M., Sticker, M., Fumagalli, S., Allegrini, P. R., Kozma, S. C., Auwerx, J. and Thomas, G. (2004) Absence of S6K1 protects against age- and diet-induced obesity while enhancing insulin sensitivity. Nature. **431**, 200-205

9 Elchebly, M., Payette, P., Michaliszyn, E., Cromlish, W., Collins, S., Loy, A. L., Normandin, D., Cheng, A., Himms-Hagen, J., Chan, C. C., Ramachandran, C., Gresser, M. J., Tremblay, M. L. and Kennedy, B. P. (1999) Increased insulin sensitivity and obesity resistance in mice lacking the protein tyrosine phosphatase-1B gene. Science. **283**, 1544-1548

10 Wong, J. T., Kim, P. T., Peacock, J. W., Yau, T. Y., Mui, A. L., Chung, S. W., Sossi, V., Doudet, D., Green, D., Ruth, T. J., Parsons, R., Verchere, C. B. and Ong, C. J. (2007) Pten (phosphatase and tensin homologue gene) haploinsufficiency promotes insulin hypersensitivity. Diabetologia. **50**, 395-403

11 Wullschleger, S., Sakamoto, K., Johnstone, L., Duce, S., Fleming, S. and Alessi, D. R. (2010) How moderate changes in Akt T-loop phosphorylation impact on tumorigenesis and insulin resistance. Dis Model Mech. **Epublished Oct 19**

12 Damen, J. E., Liu, L., Rosten, P., Humphries, R. K., Jefferson, A. B., Majerus, P. W. and Krystal, G. (1996) The 145-kDa protein induced to associate with Shc by multiple cytokines is an inositol tetraphosphate and phosphatidylinositol 3,4,5-triphosphate 5-phosphatase. Proc Natl Acad Sci U S A. **93**, 1689-1693

13 Pesesse, X., Deleu, S., De Smedt, F., Drayer, L. and Erneux, C. (1997) Identification of a second SH2-domain-containing protein closely related to the phosphatidylinositol polyphosphate 5-phosphatase SHIP. Biochem Biophys Res Commun. **239**, 697-700

14 Sleeman, M. W., Wortley, K. E., Lai, K. M., Gowen, L. C., Kintner, J., Kline, W. O., Garcia, K., Stitt, T. N., Yancopoulos, G. D., Wiegand, S. J. and Glass, D. J. (2005) Absence of the lipid phosphatase SHIP2 confers resistance to dietary obesity. Nat Med. **11**, 199-205

15 Leslie, N. R., Batty, I. H., Maccario, H., Davidson, L. and Downes, C. P. (2008) Understanding PTEN regulation: PIP2, polarity and protein stability. Oncogene. **27**, 5464-5476

16 Stephens, L. R., Jackson, T. R. and Hawkins, P. T. (1993) Agonist-stimulated synthesis of phosphatidylinositol(3,4,5)-trisphosphate: a new intracellular signalling system? Biochim Biophys Acta. **1179**, 27-75

17 Manna, D., Albanese, A., Park, W. S. and Cho, W. (2007) Mechanistic basis of differential cellular responses of phosphatidylinositol 3,4-bisphosphate- and phosphatidylinositol 3,4,5-trisphosphate-binding pleckstrin homology domains. J Biol Chem. **282**, 32093-32105

18 Dowler, S., Currie, R. A., Campbell, D. G., Deak, M., Kular, G., Downes, C. P. and Alessi, D. R. (2000) Identification of pleckstrin-homology-domain-containing proteins with novel phosphoinositide-binding specificities. Biochem J. **351**, 19-31

19 Thomas, C. C., Dowler, S., Deak, M., Alessi, D. R. and van Aalten, D. M. (2001) Crystal structure of the phosphatidylinositol 3,4-bisphosphate-binding pleckstrin homology (PH) domain of tandem PH-domain-containing protein 1 (TAPP1): molecular basis of lipid specificity. Biochem J. **358**, 287-294

20 Kimber, W. A., Trinkle-Mulcahy, L., Cheung, P. C., Deak, M., Marsden, L. J., Kieloch, A., Watt, S., Javier, R. T., Gray, A., Downes, C. P., Lucocq, J. M. and Alessi, D. R. (2002) Evidence that the tandem-pleckstrin-homology-domain-containing protein TAPP1 interacts with Ptd(3,4)P2 and the multi-PDZ-domain-containing protein MUPP1 in vivo. Biochem J. **361**, 525-536

21 Cheung, S. M., Kornelson, J. C., Al-Alwan, M. and Marshall, A. J. (2007) Regulation of phosphoinositide 3-kinase signaling by oxidants: hydrogen peroxide selectively enhances immunoreceptor-

induced recruitment of phosphatidylinositol (3,4) bisphosphate-binding PH domain proteins. Cell Signal. **19**, 902-912

22 Marshall, A. J., Krahn, A. K., Ma, K., Duronio, V. and Hou, S. (2002) TAPP1 and TAPP2 are targets of phosphatidylinositol 3-kinase signaling in B cells: sustained plasma membrane recruitment triggered by the B-cell antigen receptor. Mol Cell Biol. **22**, 5479-5491

23 Kimber, W. A., Deak, M., Prescott, A. R. and Alessi, D. R. (2003) Interaction of the protein tyrosine phosphatase PTPL1 with the PtdIns(3,4)P2-binding adaptor protein TAPP1. Biochem J. **376**, 525-535

24 Hogan, A., Yakubchyk, Y., Chabot, J., Obagi, C., Daher, E., Maekawa, K. and Gee, S. H. (2004) The phosphoinositol 3,4-bisphosphate-binding protein TAPP1 interacts with syntrophins and regulates actin cytoskeletal organization. J Biol Chem. **279**, 53717-53724

25 Costantini, J. L., Cheung, S. M., Hou, S., Li, H., Kung, S. K., Johnston, J. B., Wilkins, J. A., Gibson, S. B. and Marshall, A. J. (2009) TAPP2 links phosphoinositide 3-kinase signaling to B-cell adhesion through interaction with the cytoskeletal protein utrophin: expression of a novel cell adhesion-promoting complex in B-cell leukemia. Blood. **114**, 4703-4712

26 Hayakawa, M., Kaizawa, H., Moritomo, H., Koizumi, T., Ohishi, T., Yamano, M., Okada, M., Ohta, M., Tsukamoto, S., Raynaud, F. I., Workman, P., Waterfield, M. D. and Parker, P. (2007) Synthesis and biological evaluation of pyrido[3',2':4,5]furo[3,2-d]pyrimidine derivatives as novel PI3 kinase p110alpha inhibitors. Bioorg Med Chem Lett. **17**, 2438-2442

27 Williams, M. R., Arthur, J. S., Balendran, A., van der Kaay, J., Poli, V., Cohen, P. and Alessi, D. R. (2000) The role of 3-phosphoinositide-dependent protein kinase 1 in activating AGC kinases defined in embryonic stem cells. Curr Biol. **10**, 439-448

28 Wiggin, G. R., Soloaga, A., Foster, J. M., Murray-Tait, V., Cohen, P. and Arthur, J. S. (2002) MSK1 and MSK2 are required for the mitogen- and stress-induced phosphorylation of CREB and ATF1 in fibroblasts. Mol Cell Biol. **22**, 2871-2881

29 Ayala, J. E., Bracy, D. P., McGuinness, O. P. and Wasserman, D. H. (2006) Considerations in the design of hyperinsulinemic-euglycemic clamps in the conscious mouse. Diabetes. **55**, 390-397

30 Ayala, J. E., Bracy, D. P., Julien, B. M., Rottman, J. N., Fueger, P. T. and Wasserman, D. H. (2007) Chronic treatment with sildenafil improves energy balance and insulin action in high fat-fed conscious mice. Diabetes. **56**, 1025-1033

31 Steele, R., Wall, J. S., De Bodo, R. C. and Altszuler, N. (1956) Measurement of size and turnover rate of body glucose pool by the isotope dilution method. Am J Physiol. **187**, 15-24

32 Kraegen, E. W., James, D. E., Jenkins, A. B. and Chisholm, D. J. (1985) Dose-response curves for in vivo insulin sensitivity in individual tissues in rats. Am J Physiol. **248**, E353-362

33 Gray, A., Olsson, H., Batty, I. H., Priganica, L. and Peter Downes, C. (2003) Nonradioactive methods for the assay of phosphoinositide 3-kinases and phosphoinositide phosphatases and selective detection of signaling lipids in cell and tissue extracts. Anal Biochem. **313**, 234-245

34 Esposito, D. L., Li, Y., Cama, A. and Quon, M. J. (2001) Tyr(612) and Tyr(632) in human insulin receptor substrate-1 are important for full activation of insulin-stimulated phosphatidylinositol 3-kinase activity and translocation of GLUT4 in adipose cells. Endocrinology. **142**, 2833-2840

35 Ayala, J. E., Samuel, V. T., Morton, G. J., Obici, S., Croniger, C. M., Shulman, G. I., Wasserman, D. H. and McGuinness, O. P. (2010) Standard operating procedures for describing and performing metabolic tests of glucose homeostasis in mice. Dis Model Mech. **3**, 525-534

36 Huang, S. and Czech, M. P. (2007) The GLUT4 glucose transporter. Cell Metab. **5**, 237-252

37 Bayascas, J. R., Wullschleger, S., Sakamoto, K., Garcia-Martinez, J. M., Clacher, C., Komander, D., van Aalten, D. M., Boini, K. M., Lang, F., Lipina, C., Logie, L., Sutherland, C., Chudek, J. A., van Diepen, J. A., Voshol, P. J., Lucocq, J. M. and Alessi, D. R. (2008) Mutation of the PDK1 PH domain inhibits protein kinase B/Akt, leading to small size and insulin resistance. Mol Cell Biol. **28**, 3258-3272

38 Ooms, L. M., Horan, K. A., Rahman, P., Seaton, G., Gurung, R., Kethesparan, D. S. and Mitchell, C. A. (2009) The role of the inositol polyphosphate 5-phosphatases in cellular function and human disease. Biochem J. **419**, 29-49

39 Batty, I. H., van der Kaay, J., Gray, A., Telfer, J. F., Dixon, M. J. and Downes, C. P. (2007) The control of phosphatidylinositol 3,4-bisphosphate concentrations by activation of the Src homology 2 domain containing inositol polyphosphate 5-phosphatase 2, SHIP2. Biochem J. **407**, 255-266

40 Erdmann, K. S. (2003) The protein tyrosine phosphatase PTP-Basophil/Basophil-like. Interacting proteins and molecular functions. Eur J Biochem. **270**, 4789-4798

41 Adachi, M., Hamazaki, Y., Kobayashi, Y., Itoh, M., Tsukita, S. and Furuse, M. (2009) Similar and distinct properties of MUPP1 and Patj, two homologous PDZ domain-containing tight-junction proteins. Mol Cell Biol. **29**, 2372-2389

42 Haenggi, T. and Fritschy, J. M. (2006) Role of dystrophin and utrophin for assembly and function of the dystrophin glycoprotein complex in non-muscle tissue. Cell Mol Life Sci. **63**, 1614-1631

43 Villa, F., Deak, M., Bloomberg, G. B., Alessi, D. R. and van Aalten, D. M. (2005) Crystal structure of the PTPL1/FAP-1 human tyrosine phosphatase mutated in colorectal cancer: evidence for a second phosphotyrosine substrate recognition pocket. J Biol Chem. **280**, 8180-8187

44 Salmeen, A., Andersen, J. N., Myers, M. P., Tonks, N. K. and Barford, D. (2000) Molecular basis for the dephosphorylation of the activation segment of the insulin receptor by protein tyrosine phosphatase 1B. Mol Cell. **6**, 1401-1412

45 Miao, B., Skidan, I., Yang, J., Lugovskoy, A., Reibarkh, M., Long, K., Brazell, T., Durugkar, K. A., Maki, J., Ramana, C. V., Schaffhausen, B., Wagner, G., Torchilin, V., Yuan, J. and Degterev, A. (2010) Small molecule inhibition of phosphatidylinositol-3,4,5-triphosphate (PIP3) binding to pleckstrin homology domains. Proc Natl Acad Sci U S A. **107**, 20126-20131

Figure legends

Figure 1
Generation and analysis of TAPP1$^{R211L/R211L}$ and TAPP2$^{R218L/R218L}$ knock-in mice.
(A) Diagram depicting the knock-in construct, the endogenous TAPP1 allele containing exons 4-9 and the targeted allele with the neomycin cassette removed by Flp recombinase. The black/grey rectangles represent exons, the grey triangles represent *FRT* sites and the black triangles represent *LOX P* sites. (B) To confirm correct vector insertion genomic DNA purified from the targeted ES cells was digested with either *HpaI* or *KpnI* and subjected to Southern blot analysis. (C) To genotype mice genomic DNA was PCR amplified with primers P1 and P2. (D) Genomic DNA obtained from mice was subjected to PCR to generate a product encompassing the knock-in mutation region. To verify the presence of the knock-in mutation the PCR products were sequenced and the wild-type and knock-in sequences are presented. (E) Diagram depicting the knock-in construct, the endogenous TAPP2 allele containing exons 4-10 and the targeted allele with the neomycin cassette removed by Flp recombinase. (F) To confirm correct vector insertion genomic DNA purified from the targeted ES cells was digested with either *XhoI* or *EcoRV* and subjected to Southern blot analysis. (G) To genotype mice genomic DNA was PCR amplified with primers P1 and P2. (H) Genomic DNA obtained from mice was amplified by PCR to generate a product encompassing the knock-in mutation region. To verify the presence of the knock-in mutation PCR products were sequenced and the wild-type and knock-in sequences are presented.

Figure 2
Analysis of TAPP1$^{R211L/R211L}$ TAPP2$^{R218L/R218L}$ double knock-in mice.
(A) Tissue lysates from wild-type TAPP1$^{+/+}$ TAPP2$^{+/+}$ and TAPP1$^{R211L/R211L}$ TAPP2$^{R218L/R218L}$ double knock-in mice were subjected to immunoblot analysis using TAPP1, TAPP2 and GAPDH antibodies. (B) PtdIns(3,4)P_2 -agarose pull-downs of lung extracts from wild-type TAPP1$^{+/+}$ TAPP2$^{+/+}$ (WT) and TAPP1$^{R211L/R211L}$ TAPP2$^{R218L/R218L}$ (R211L)mice and total lysates were subjected to immunoblot analysis using TAPP1 antibody. (C) PtdIns(3,4)P_2 -agarose pull-downs of spleen extracts from wild-type TAPP1$^{+/+}$ TAPP2$^{+/+}$ (WT) and TAPP1$^{R211L/R211L}$ TAPP2$^{R218L/R218L}$ (R218L) mice and total lysates were subjected to immunoblot analysis using TAPP2 antibody. (D) The body weight of wild-type TAPP1$^{+/+}$ TAPP2$^{+/+}$ and TAPP1$^{R211L/R211L}$ TAPP2$^{R218L/R218L}$ double knock-in mice was monitored over a period of 16 weeks. Body weight is depicted as mean±SEM of males (left panel) and females (right panel) animals (TAPP1$^{+/+}$ TAPP2$^{+/+}$ n=12, TAPP1$^{R211L/R211L}$ TAPP2$^{R218L/R218L}$ n=10). (E) Blood glucose and plasma insulin F) levels of fed and over night fasted wild-type TAPP1$^{+/+}$ TAPP2$^{+/+}$ and TAPP1$^{R211L/R211L}$ TAPP2$^{R218L/R218L}$ knock-in mice. Data are presented as mean±SEM of male mice, 3 months of age (TAPP1$^{+/+}$ TAPP2$^{+/+}$ n=10, TAPP1$^{R211L/R211L}$ TAPP2$^{R218L/R218L}$ n=10).

Figure 3
Increased Akt activation in TAPP1$^{R211L/R211L}$ TAPP2$^{R218L/R218L}$ double knock-in mice upon insulin stimulation.
Wild-type TAPP1$^{+/+}$ TAPP2$^{+/+}$ and TAPP1$^{R211L/R211L}$ TAPP2$^{R218L/R218L}$ double knock-in male mice, 3 months of age, were starved for 5 hrs and injected (i.v.) with insulin (1 mU/g body weight) for 20 min. Tissue extracts of liver (A), heart (B) and gastrocnemius muscle (C) were generated and analysed by immunoblotting using the indicated antibodies. Samples from every lane in each blot shown are derived from a separate mouse. Akt was also immunoprecipitated and its activity in the different tissues measured by in vitro kinase assay (*$p<0.05$, n=3-4). The data is presented as average (mU/mg) ± SEM.

Figure 4
Enhanced insulin sensitivity and glucose metabolic index in TAPP1$^{R211L/R211L}$ TAPP2$^{R218L/R218L}$ double knock-in mice.
(A) Glucose infusion rates in wild-type TAPP1$^{+/+}$ TAPP2$^{+/+}$ and TAPP1$^{R211L/R211L}$ TAPP2$^{R218L/R218L}$ double knock-in male mice, 6 months of age, during hyerinsulinemic-euglycemic clamp study. Area under curve (AUC) for glucose infusion rates at steady state (80 min to 120 min) was determined (**P<0.004). (B) Whole body glucose disappearance rates (R_d) of wild-type TAPP1$^{+/+}$ TAPP2$^{+/+}$ and TAPP1$^{R211L/R211L}$ TAPP2$^{R218L/R218L}$ double knock-in mice under basal and clamp conditions (*P<0.02). (C) Endogenous glucose appearance rate ($EndoR_a$) of wild-type TAPP1$^{+/+}$ TAPP2$^{+/+}$ and TAPP1$^{R211L/R211L}$ TAPP2$^{R218L/R218L}$ double knock-in mice under basal and clamp conditions. (D) 2-deoxyglucose uptake during the clamp was determined in adipose, gastrocnemius muscle, diaphragm and heart tissues of wild-type TAPP1$^{+/+}$ TAPP2$^{+/+}$ (TAPP1/2 Wt) and TAPP1$^{R211L/R211L}$ TAPP2$^{R218L/R218L}$ (TAPP1/2 Ki) double knock-in mice (**P<0.005 gastrocnemius muscle, *p<0.01 heart). TAPP1$^{+/+}$ TAPP2$^{+/+}$ n=7, TAPP1$^{R211L/R211L}$ TAPP2$^{R218L/R218L}$ n=8 for (A)-(D).

Figure 5
Increased PtdIns(3,4,5)P_3 production and Akt activation in TAPP1$^{R211L/R211L}$ TAPP2$^{R218L/R218L}$ double knock-in MEF cells upon insulin stimulation.
Mouse embryonic fibroblasts (MEF) cells derived from wild-type TAPP1$^{+/+}$ TAPP2$^{+/+}$ and TAPP1$^{R211L/R211L}$ TAPP2$^{R218L/R218L}$ double knock-in mice were serum-starved over night. Cells were left untreated or treated with 1 μM PI-103 or 10 nM insulin for the indicated time. (A) PtdIns(3,4,5)P_3 levels expressed as pmol per mg of cellular protein were quantified. The data shows average values for a triplicate experiment ± SEM. Similar results were obtained in two separate experiments. (B) Akt was immunoprecipitated and activity measured by in vitro kinase assay (*p<0.05, n=3-4). The data is presented as average activity (mU/mg) ± SEM. Cell extracts were analysed by immunoblotting using the indicated antibodies. Samples from every lane in each blot shown are derived from a separate cell dish.

Table 1
Breeding strategy used to generate TAPP1$^{R211L/R211L}$, TAPP2$^{R218L/R218L}$ and TAPP1$^{R211L/R211L}$TAPP2$^{R218L/R218L}$ knock-in mice.
Single homozygous TAPP1$^{R211L/R211L}$ and TAPP2$^{R218L/R218L}$, as well as double TAPP1$^{R211L/R211L}$TAPP2$^{R218L/R218L}$ knock-in mice, were bred using the strategy depicted in Table 1 and the progeny was genotyped as described in the methods. The number and the percentage of each genotype are indicated followed by its expected Mendelian frequency. In the case of the double TAPP1$^{R211L/R211L}$TAPP2$^{R218L/R218L}$ knock-in mice, as wild-type littermate and double knock-in mice can only be obtained at a ratio of 1 in 16 in the same cross (Table 1), we interbred TAPP1$^{R211L/R211L}$TAPP2$^{R218L/R218L}$ and TAPP1$^{R211L/R211L}$TAPP2$^{R218L/R218L}$ as well as TAPP1$^{+/+}$TAPP2$^{+/+}$ and TAPP1$^{+/+}$TAPP2$^{+/+}$ littermates derived from a 1 in 16 ratio mating.

Biochemical Journal Immediate Publication. Published on 04 Jan 2011 as manuscript BJ20102012

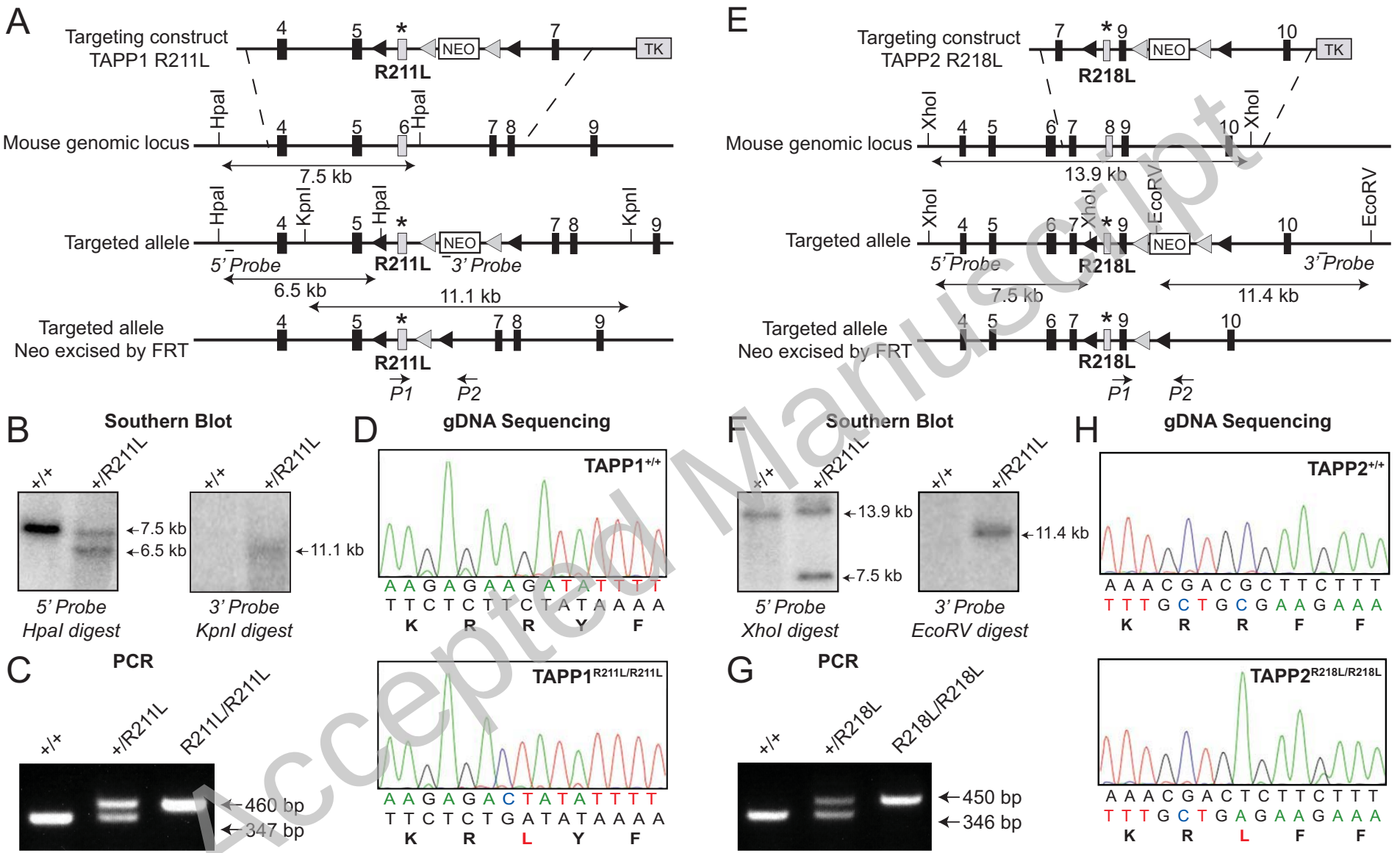

Figure 1

Biochemical Journal Immediate Publication. Published on 04 Jan 2011 as manuscript BJ20102012

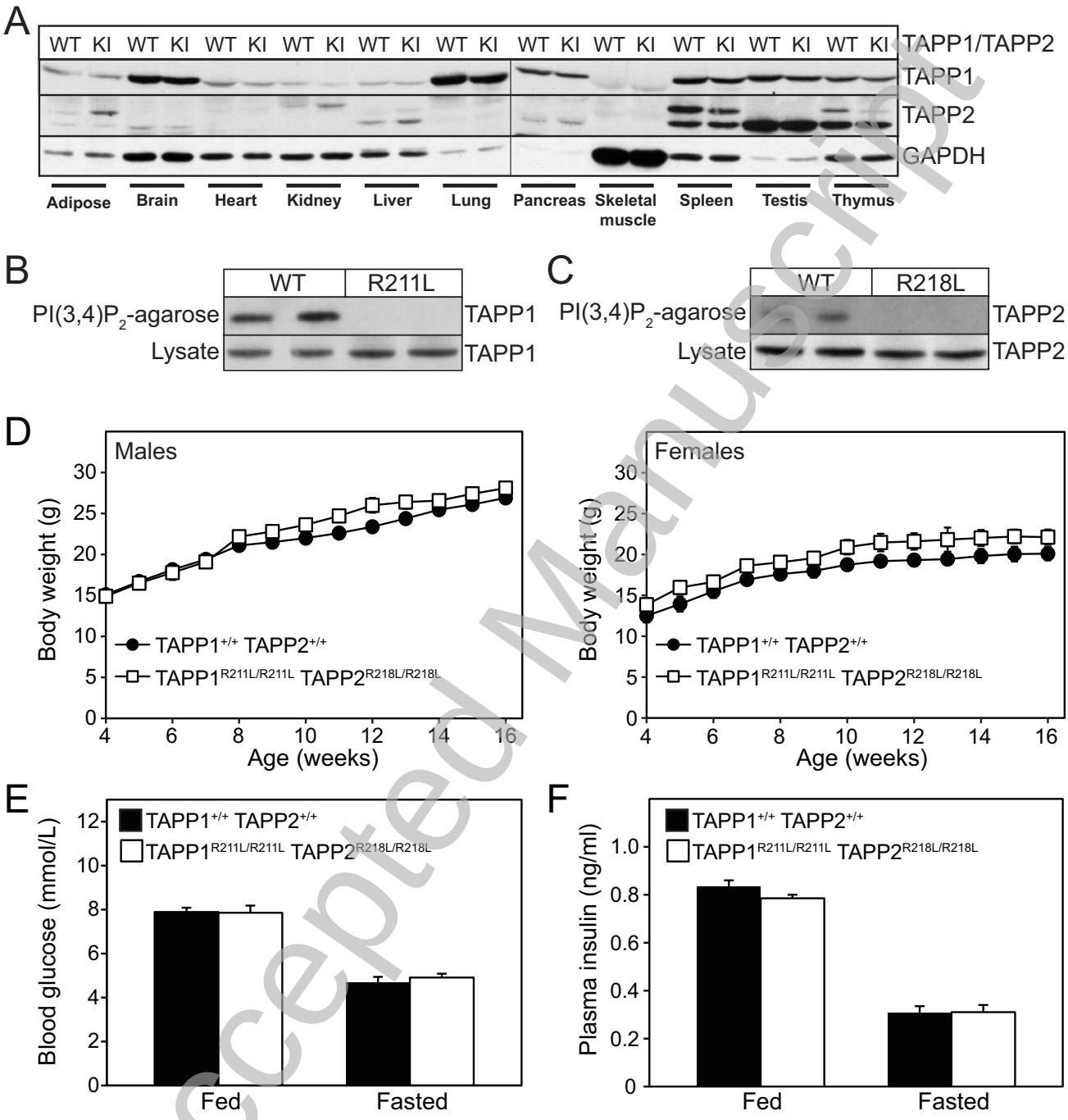

Figure 2

Biochemical Journal Immediate Publication. Published on 04 Jan 2011 as manuscript BJ20102012

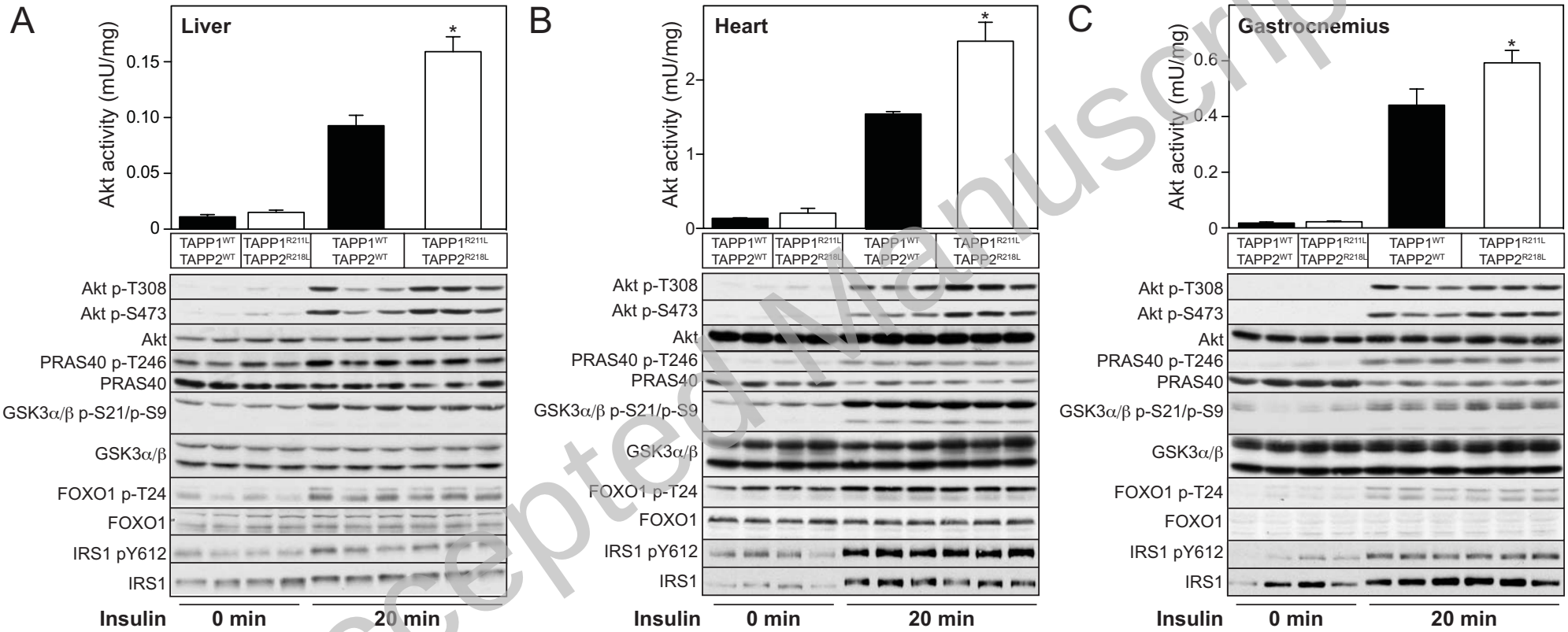

Figure 3

Biochemical Journal Immediate Publication. Published on 04 Jan 2011 as manuscript BJ20102012

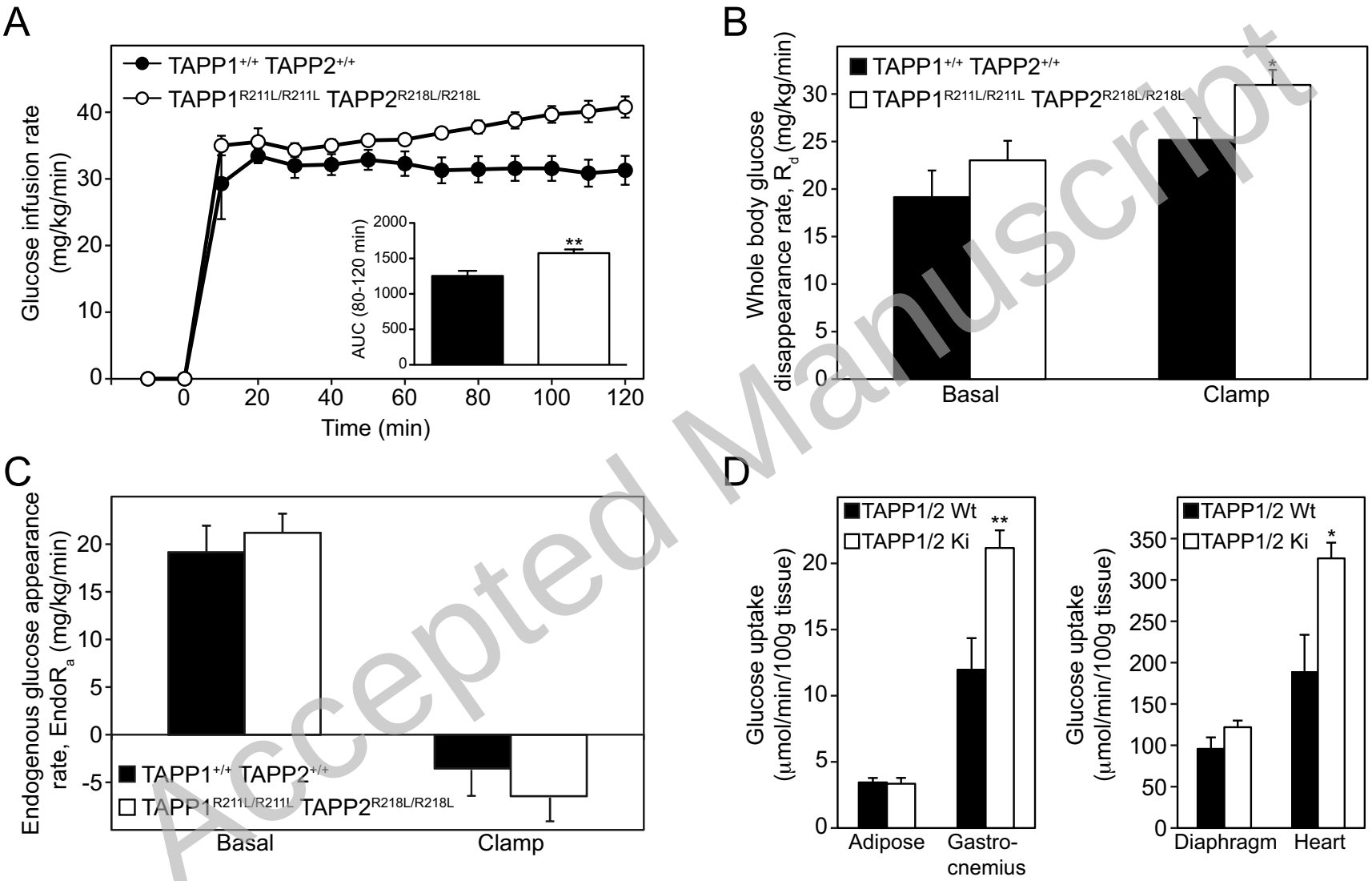

Figure 4

Biochemical Journal Immediate Publication. Published on 04 Jan 2011 as manuscript BJ20102012

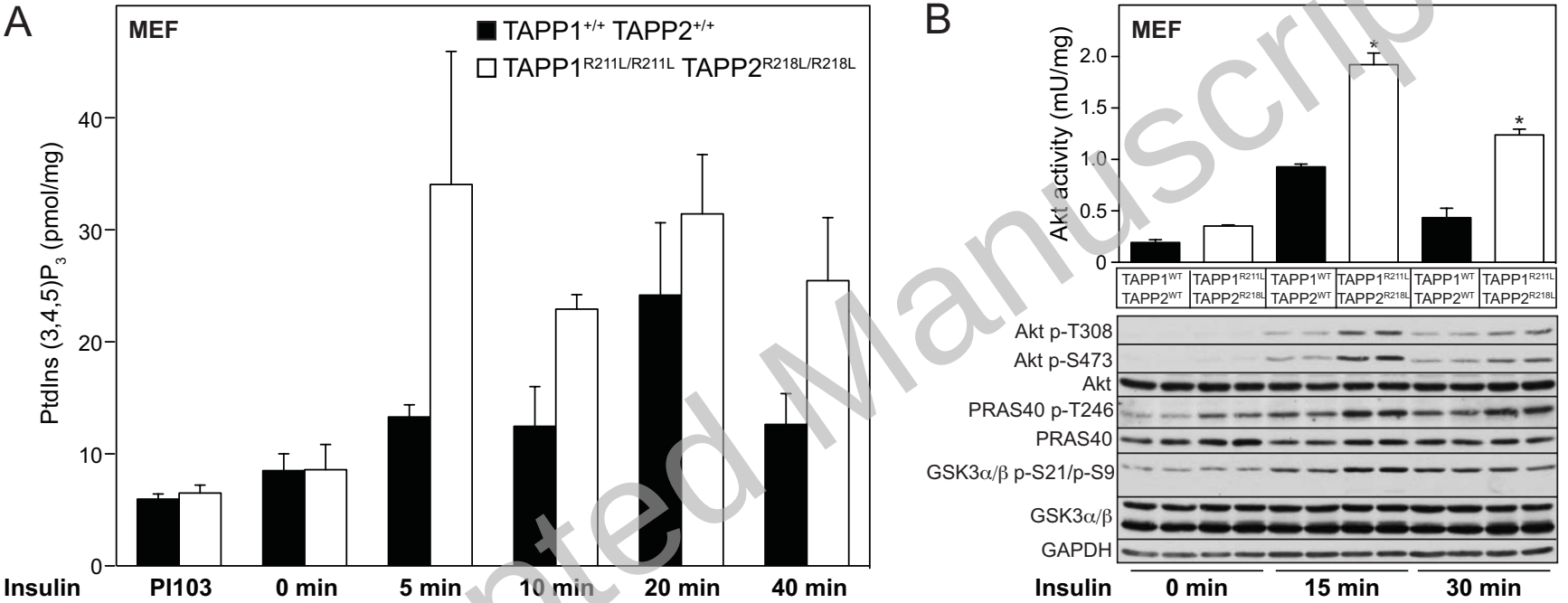

Figure 5

Cross	Genotype	Number born	Expected Mendelian Frequency
$TAPP1^{+/R211L}$ $TAPP1^{+/R211L}$	$TAPP1^{+/+}$	11 (24.45%)	25%
	$TAPP1^{+/R2111L}$	23 (51.1%)	50%
	$TAPP1^{R211L/R211L}$	11 (24.45%)	25%
$TAPP2^{+/R218L}$ $TAPP2^{+/R218L}$	$TAPP2^{+/+}$	21 (31.8%)	25%
	$TAPP2^{+/R218L}$	28 (42.4%)	50%
	$TAPP2^{R218L/R218L}$	17 (25.8%)	25%
$TAPP1^{+/R211L}$ $TAPP2^{+/R218L}$ $TAPP1^{+/R211L}$ $TAPP2^{+/R218L}$	$TAPP1^{+/+}$ $TAPP2^{+/+}$	6 (5.7%)	6.25%
	$TAPP1^{R211L/R211L}$ $TAPP2^{R218L/R218L}$	5 (4.8%)	6.25%
	$TAPP1^{+/R211L}$ $TAPP2^{+/R218L}$	28 (26.7%)	25%
	$TAPP1^{+/R211L}$ $TAPP2^{+/+}$	19 (18.1%)	12.5%
	$TAPP1^{+/+}$ $TAPP2^{+/R218L}$	14 (13.3%)	12.5%
	$TAPP1^{R211L/R211L}$ $TAPP2^{+/+}$	4 (3.8%)	6.25%
	$TAPP1^{+/+}$ $TAPP2^{R218L/R218L}$	5 (4.8%)	6.25%
	$TAPP1^{R211L/R211L}$ $TAPP2^{+/R218L}$	14 (13.3%)	12.5%
	$TAPP1^{+/R211L}$ $TAPP2^{R218L/R218L}$	10 (9.5%)	12.5%
$TAPP1^{+/+}$ $TAPP2^{+/+}$ $TAPP1^{+/+}$ $TAPP2^{+/+}$	$TAPP1^{+/+}$ $TAPP2^{+/+}$	100%	
$TAPP1^{R211L/R211L}$ $TAPP2^{R218L/R218L}$ $TAPP1^{R211L/R211L}$ $TAPP2^{R218L/R218L}$	$TAPP1^{R211L/R211L}$ $TAPP2^{R218L/R218L}$	100%	

Table 1